Applied Surface Science 378 (2016) 496–503

Contents lists available at ScienceDirect

Applied Surface Science

journal homepage: www.elsevier.com/locate/apsusc

Facile incorporation of hydroxyapatite onto an anodized Ti surface via a mussel inspired polydopamine coating

Zhe Wang[a], Chaofang Dong[a,*], Sefei Yang[b], Dawei Zhang[a], Kui Xiao[a], Xiaogang Li[a]

[a] Corrosion and Protection Center, Key Laboratory for Corrosion and Protection (MOE), University of Science and Technology Beijing, Beijing 100083, China
[b] Department of Stomatology, The PLA General Hospital, Beijing, China

ARTICLE INFO

Article history:
Received 22 November 2015
Received in revised form 6 February 2016
Accepted 11 March 2016
Available online 14 March 2016

Keywords:
Ti
Polydopamine
Hydroxyapatite
Corrosion resistance
Biocompatibility

ABSTRACT

Inspired by the porous morphology of anodized Ti and the adhesive versatility of polydopamine (PDA), which can induce apatite mineralization, we fabricated a novel interface by coating a porous anodized TiO_2 layer with PDA to rapidly immobilize HA on Ti-based substrates. It was found that the as-prepared PDA/anodized (HD) surface exhibited nanoscale roughness, which possessed an excellent ability to form apatite when immersed in 1.5× simulated body fluid (SBF), as observed by AFM and FE-SEM. The morphology and composition of each layer were further confirmed by XPS, XRD and FTIR. The corrosion resistance of the multilayer was investigated using potentiodynamic polarization curve and electrochemical impedance spectra (EIS) measurements in a 0.9 wt% NaCl solution, the results suggested that the HA/PDA/anodized (HDA) layer increased the corrosion resistance of pure Ti with higher corrosion potential and lower passive current, the surface wettability was also enhanced with the incorporation of HA. In vitro cellular assays showed that the HDA layer stimulated cell attachment and improved the alkaline phosphate (ALP) activity. Overall, the PDA/anodized treatment provided a viable method to quickly integrate HA, and the obtained HDA layer improved both corrosion resistance and biocompatibility of the Ti surface.

1. Introduction

Commercially pure titanium and its alloys are widely used as dental and orthopaedic implants due to their favorable mechanical properties and chemical stability. However, the natural TiO_2 layer that forms in the atmosphere is bio-inert, which leads to mechanical interlocking between the implant surface and bone tissues [1]. Thus, numerous attempts have been made to modify the composition and topography of the implant surfaces for a quicker fixation. Among various coating methods, anodic oxidation is a classical method for modifying the surface structure. This technique can produce a uniformly porous and dense TiO_2 layer with good adhesion properties, which not only enhance osseointegration, but also largely improve the corrosion resistance in vivo [2,3]. However, ideal implant surfaces always mimic the morphology and components of natural bone. Therefore, various organic or inorganic substances, such as peptide RGD [4], bone morphogenetic proteins (BMP) [5,6] and hydroxyapatite [7–9] are immobilized on the implant surface to obtain a better biocompatibility.

Hydroxyapatite coating has been a common strategy to improve osteointegration for dental and orthopaedic implants because of its similarity in chemistry and structure to the inorganic component of natural bone. Therefore, several techniques, such as plasma spraying, sol-gel, sputtering [10–12] and an electrophoretic deposition-coupled micro-arc [13], have been explored to accomplish this goal. Nevertheless, these techniques often require complex chemical syntheses or costly devices with enormous loss of energy and time. To overcome these drawbacks, efforts are currently aimed at mimicking biomineralization phenomena to synthesize HA in situ with low-energy consumption [14].

Inspired by the adhesive protein in mussels [15], Lee et al. have developed a facile approach to modify a wide variety of materials by the polymerization of dopamine. In the presence of O_2 and an alkaline Tris–HCl solution was employed as a medium, the dopamine molecules were oxidized, cyclized intramolecularly and self-polymerized to form particles, these particles then aggregated and grew into a thin polydopamine film with large numbers of bioactive groups exposed [16], such as —OH and —NH_2, which created an effective platform for further modification. In particular, when the coating was dipped into simulated body fluid (SBF), it spontaneously induced apatite mineralization [17], whereby SBF

* Corresponding author.
E-mail address: cfdong@ustb.edu.cn (C. Dong).

http://dx.doi.org/10.1016/j.apsusc.2016.03.094
0169-4332/

provided Ca and P ions, and polydopamine provided the nucleation sites for mineralization.

Polydopamine, an adherent coating on various materials, provides a universal route to integrate inorganic hydroxyapatite crystals with versatile materials. Yuntao Wu et al. [18] have modified Ti substrates through layer-by-layer assembly of PDA and HA, and the hybrid layer showed outstanding interfacial stability and good bioactivity. However, this method required an alternate immersion of substrates in dopamine and 1.5× SBF solutions for several times, which was tedious and complex. Additionally, a two-week immersion in a 1.5× SBF solution was needed to form a uniform Ca-P mineral film on smooth PDA-coated Ti substrates [17]. Thus, a simple and rapid method to immobilize HA on PDA is highly desired. Inspired by the flexible coating character of PDA, which can modify the inner surface of porous materials [17,19], we attempt to introduce a PDA layer to anodized Ti surface. Because the porous layer can increase the surface area, and a rougher surface is always easier for heterogeneous nucleation [20], we hypothesized that the PDA/anodized layer could exhibit a greater affinity for HA. Furthermore, the composite coating would improve both the corrosion resistance and the cell response in biological environments.

In the present study, self-polymerized dopamine nucleated on the surface of anodized Ti substrates, which were submerged into 1.5× SBF to test the growth rate of HA. This growth was then compared with that on other types of substrates (uncoated Ti, anodized Ti and PDA coated Ti). Moreover, the chemical composition, morphology and hydrophilicity of each layer were investigated. Finally, the corrosion resistance and the biological effects of each layer on MC3T3-E1 cells were studied.

2. Materials and methods

2.1. Materials

Commercial pure titanium disks (diameter: 15 mm and thickness: 1 mm) were used as substrates. The samples were sequentially ground using SiC paper from #400 to #2000, degreased with acetone, ultrasonically washed in ethanol and deionized water, and finally dried in air.

2.2. TiO_2 porous film fabrication

The TiO_2 porous film was prepared by applying a pulsed DC field to specimen using a pulsed DC power supply. The frequency and duty cycle of the pulsed DC power were 550 Hz and 90%. Titanium foil was used as the positive electrode and platinum foils were employed as negative electrodes. The samples were anodized in a 1 M H_2SO_4 electrolyte for 1 min at room temperature [21]. The uncoated Ti and the anodized Ti are designated as Ti and H-Ti, respectively.

2.3. Polydopamine-assisted hydroxyapatite formation

The PDA-coated substrates were prepared as described by Lee et al. [15]. The uncoated Ti and the H-Ti specimens were immersed in a solution of 10 mM Tris-HCl adjusted to pH 8.5, and then, dopamine at a concentration of 2 mg ml^{-1} was added. Before being magnetically stirred and to ensure that the interior surface of microporous TiO_2 was modified, the coating solution was dispersed by ultrasonication. After soaking for 24 h, the prepared substrates were rinsed with deionized water, immersed into 1.5× SBF and incubated, at 37 °C for 48 h to form hydroxyapatite. For comparison, the Ti and the H-Ti groups were also dipped into 1.5× SBF in the same condition, and each group had five specimens to ensure the results reliable. The SBF solution was prepared according to the previous report by Kokubo [22] with ion concentrations (Na^+ 213, K^+ 7.5, Mg^{2+} 2.25, Ca^{2+} 3.75, Cl^- 221.7, HCO_3^- 6.3, HPO_4^{2-} 1.5 and SO_4^{2-} 0.75 mM) nearly 1.5 times that of human blood plasma at pH 7.40. The PDA/anodized Ti and HA/PDA/anodized Ti are referred to HD-Ti and HDA-Ti, respectively.

2.4. Surface characterization

The surface morphology and microstructure of the specimens were observed by a field-emission scanning electron microscope (FE-SEM, Quanta 450, FEI). Atomic force microscopy (AFM, Multimode, Bruker) was used to detect the morphology and surface roughness of PDA films grown on silicon substrates using the tapping mode with a scanning frequency of 1 Hz. Micro-Fourier transform infrared (FTIR, spotlight 200, PE, USA) spectra were recorded from 2000 to 650 cm^{-1} to analyse the components of the surface. The elemental composition of each layer was determined by X-ray photoelectron spectroscopy (XPS, ESCALAB250, Thermo Fisher) with a monochromatic Al Kα source (100 eV). The crystal structures of anodic TiO_2 and the HA layer that formed on the titanium surface were examined by thin film X-ray diffraction (TF-XRD, Ultima IV, Rigaku, Japan) using a Cu Kα radiation generated at 45 kV and 200 mA. The static water contact angle was estimated with a contact angle measurement (OCA 20, Data Physics, Germany) using a water drop volume of 2 μl. The mean value of each substrate was determined by measuring different samples at least five times.

2.5. Corrosion resistance

Potentiodynamic polarization was carried out to assess the corrosion performance of uncoated Ti and HD-Ti using an AutoLab electrochemical workstation (Metrohm PGSTAT302N, Switzerland) with a traditional three-electrode cell. The test specimens were used as working electrodes, while a platinum plate and a saturated calomel electrode (SCE) were used as the counter and reference electrodes, respectively. Before the tests began, the specimens were immersed into the electrolyte for 30 min to remain electrochemical stabilities, then the open circuit potentials (OCP) were conducted, after the OCP fluctuations were within 10 μV/s, the electrochemical impedance spectroscopy (EIS) was studied in a frequency range of 10^4–10^{-2} Hz with the perturbation amplitude of 10 mV. The polarization curves were measured at a scan rate of 1 mV/s, from −1500 mV to +1500 mV vs. SCE. The electrolyte was a 0.9 wt% NaCl solution maintained at room temperature. Although some researchers have reported the corrosion behavior of Ti and its alloys at body temperature [23,24] in recent reviews and reports, Upadhyay et al. [25] have compiled many reports in terms of the test temperature, which suggests that it is reasonable to evaluate the corrosion behavior of Ti at room temperature. The test for each condition was repeated at least three times to insure data reliability.

2.6. The biological effect on MC3T3-E1 cells

The biological effects, including cell adhesion and alkaline phosphate (ALP) activity, of different specimens on MC3T3-E1 cells were investigated in this study. The MC3T3-E1 cell line was obtained from the Cell Resource Center, Peking Union Medical College.

The immunofluorescent staining technique was used for the cell adhesion assay. The MC3T3-E1 cells were cultured on the test Ti specimens with an initial cell seeding density of 3×10^4 cells/well (24-well plate), each group had three samples. After 2 days of culture, the MC3T3 cells adhered to substrates were fixed with 4% paraformaldehyde (Sinopharm, China) and permeabilized with 0.5% Triton X-100 (Applichem, Germany) in phosphate buffered saline (PBS). Then, the treated samples were washed with PBS and incubated with 5% normal non-immunological goat serum (Dingguo Changsheng biotechnology Co., Ltd., China). After that, the

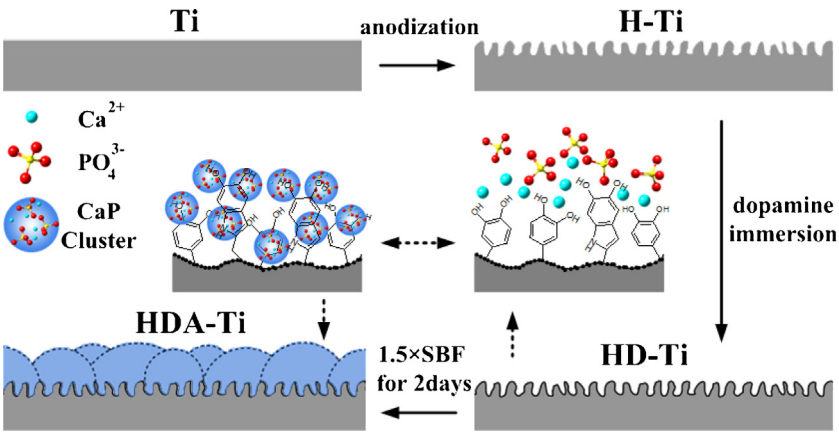

Fig. 1. The illustration of the formation mechanism of PDA-assisted HA onto anodized Ti substrates.

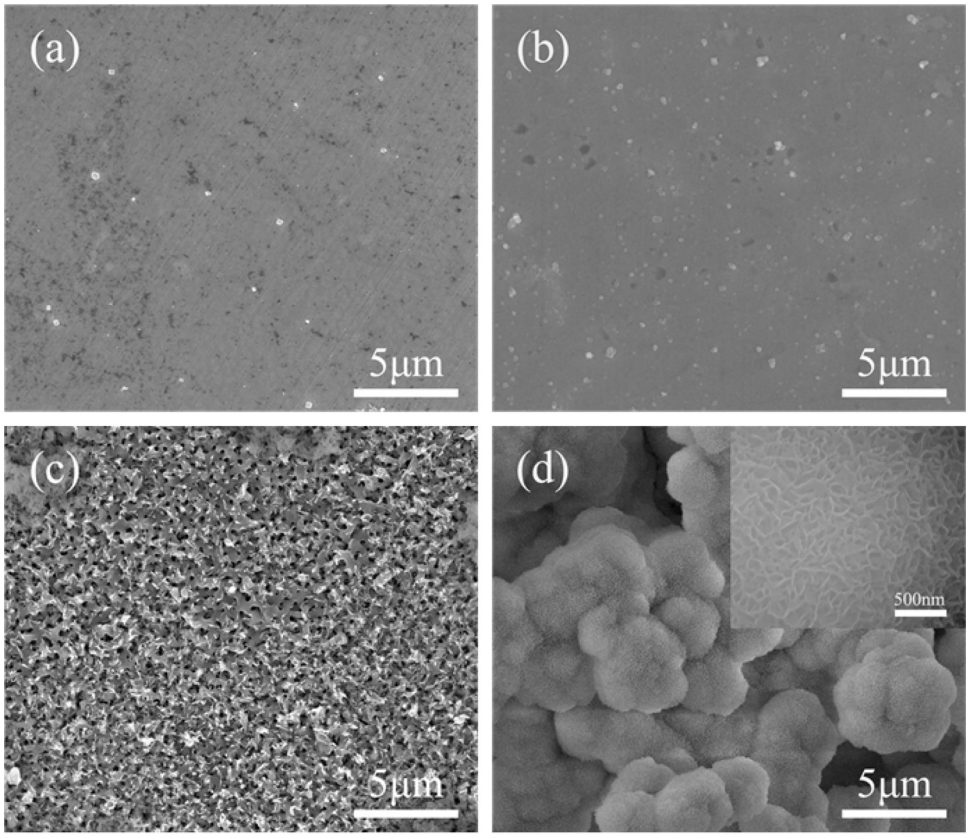

Fig. 2. Surface micrographs of specimens after immersed in 1.5× SBF for 2 days:(a) Ti, (b) D-Ti, (c) H-Ti and (d) HD-Ti.

cells subjected to mouse monoclonal anti-vinculin (Abcam, England) at 4 °C overnight. Subsequently, a mouse-antigoat tetraethyl rhodamine isothiocyanate (TRITC)-conjugated secondary antibody (1:50, Jackson ImmunoResearch, USA) was added at 37 °C for another 1 h. Finally, the F-actin and the nuclei were stained with fluorescein isothiocyanate (FITC)-phalloidin (Sigma-Aldrich, USA) and 4′,6-diamidino-2-phenylindole (DAPI, Sigma-Aldrich, USA), respectively. Cell images were observed with CLSM (TCS SP8, Leica, Germany).

The alkaline phosphate activity (ALP), an early marker of the maintenance of the osteoblastic phenotype, was measured by an ALP assay kit (Beyotime, China) to detect the degree of osteogenic differentiation. P-nitrophenyl phosphate (PNPP) was employed to determine the ALP activity of MC3T3-E1 cells cultured on different modified substrates, which was based on the theory that PNPP can be converted to *p*-nitrophenol (PNP) in the presence of ALP and the production of PNP was proportional to the ALP activity. The ALP activity was tested by the absorbance at wavelength of 405 nm using a spectrophotometric microplate reader (Multiskan MK3, Thermo), and the results were normalized by the total intracellular protein production (μmol/min/g protein). The tests were repeated twice, and each condition had three samples involved.

3. Results and discussion

Fig. 1 shows the process of PDA-assisted hydroxyapatite formation on porous TiO_2 substrates. First, a TiO_2 porous film was fabricated by anodization in a H_2SO_4 solution. Then, the prepared

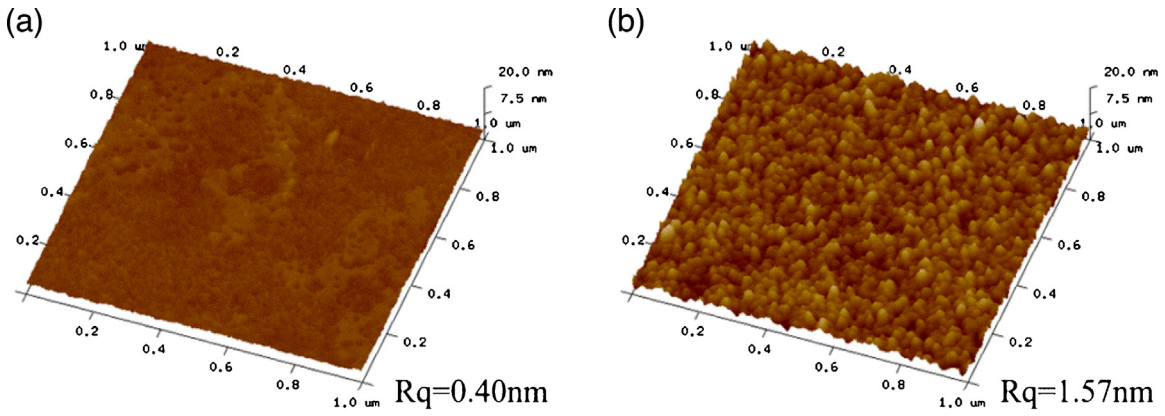

Fig. 3. AFM topography images and roughness of specimens: (a) silicon and (b) PDA-coated silicon.

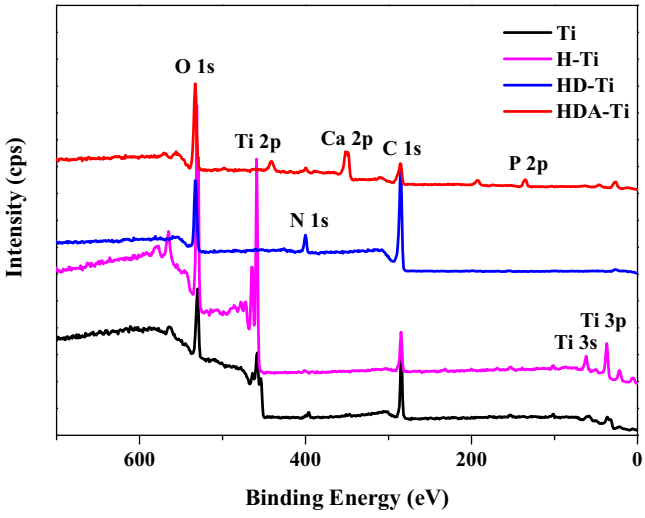

Fig. 4. XPS spectra of Ti, H-Ti, HD-Ti and HDA-Ti surface..

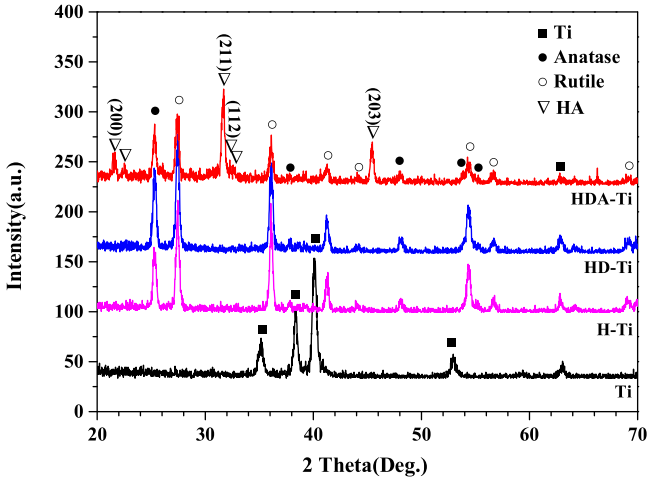

Fig. 5. TF-XRD patterns of Ti, H-Ti, HD-Ti and HDA-Ti.

porous TiO_2 substrates were dipped into a dopamine solution, forming the polydopamine film. Finally, the modified substrates were immersed into 1.5× SBF to form hydroxyapatite.

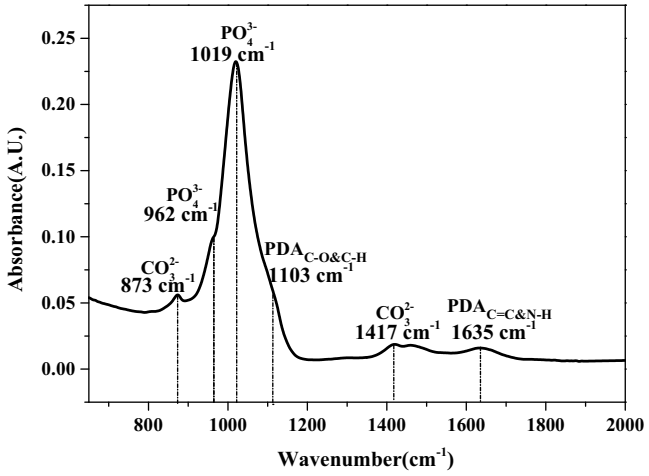

Fig. 6. FT-IR spectra of HDA-Ti.

3.1. Surface characterization

Fig. 2 presents the surface morphologies of the specimens used in this study. Uncoated titanium (Ti), PDA-coated titanium (D-Ti), anodized titanium (H-Ti) and PDA/anodized Ti (HD-Ti) were immersed into 1.5× SBF at 37 °C for 2 days (Fig. 1a–d). Compared with the three other treatment groups, the HD-Ti displays the best apatite growth, and the high-magnification SEM image shows a lath-like structure of agglomerates, which is the typical form of hydroxyapatite crystals [17]. This result was attributed to factors that influence heterogeneous nucleation, including surface structural characteristics, interfacial molecular recognition and so on [26,27]. In this study, PDA-modified substrates promoted the hydroxyl functionalization of surfaces, the numerous —OH attracted calcium (Ca^{2+}), and then bonded with the phosphate (PO_4^{3-}) and carbonic acid (CO_3^{2-}) ions in the SBF. With the immersion time extended, the degree of supersaturation in the vicinity of the —OH group increased, which triggered the nucleation of apatite. The surface topography of HD-Ti also contributed to the nucleation. Primarily, the anodized porous substrates increased the surface area, which consequently provided abundant hydroxyl groups and nucleation sites. Additionally, the morphology of the PDA layer enhanced the growth of apatite. This layer was formed by the aggregation of massive PDA particles [28], therefore, the surface coating with PDA was always concavo-convex. We verified this by analysing PDA coatings onto silicon substrates by AFM, as shown in Fig. 3. Compared with the 0.40 nm roughness of the uncoated silicon, the PDA coated silicon possessed a more textured surface with

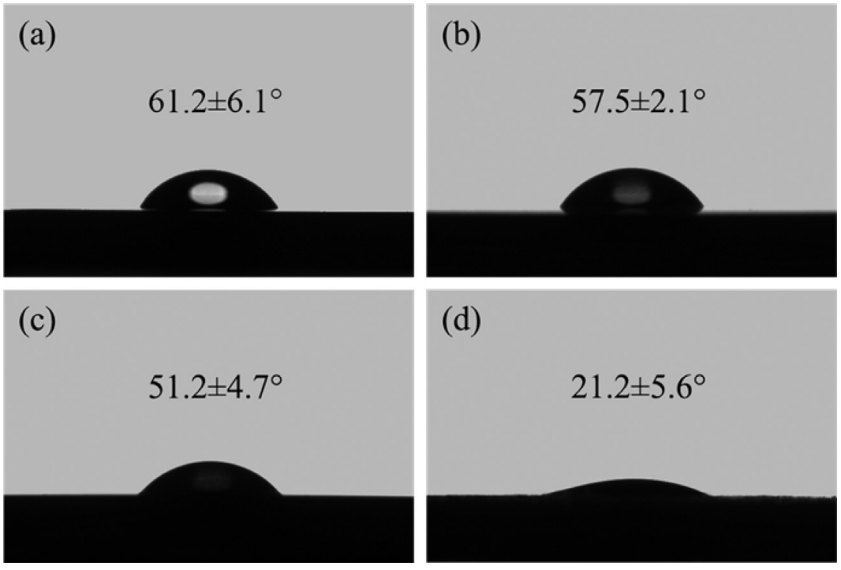

Fig. 7. Water contact angle of all specimens in the study: (a) Ti, (b) H-Ti, (c) HD-Ti and (d) HDA-Ti.

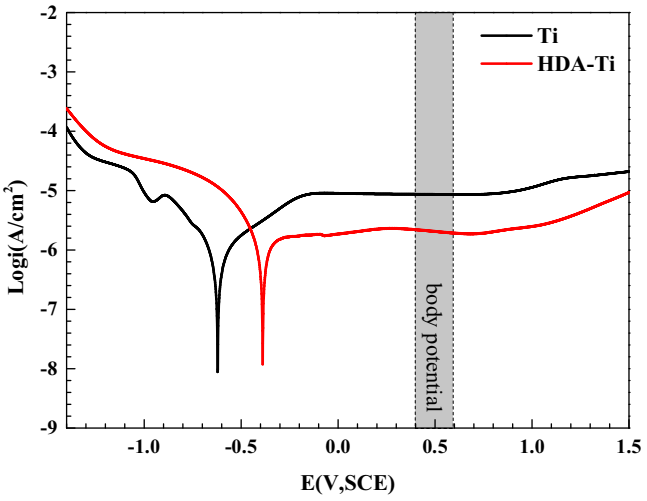

Fig. 8. Potentiodynamic polarization curves of the Ti and HDA-Ti specimens in 0.9 wt% NaCl solution.

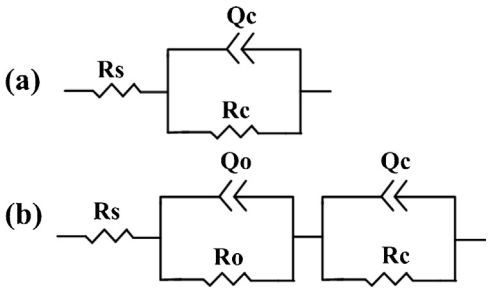

Fig. 10. The equivalent circuits for different surfaces: (a) Ti and (b) HDA-Ti.

a roughness of 1.57 nm. Increasing the surface roughness always decreases the energetic barrier to heterogeneous nucleation [20], the depressions in the morphology can prevent the initial growth of clusters and hinder random migration over the surface. Thus, clusters soon become trapped between the convex and concave regions, aggregate and grow into several large nuclei and later crys-

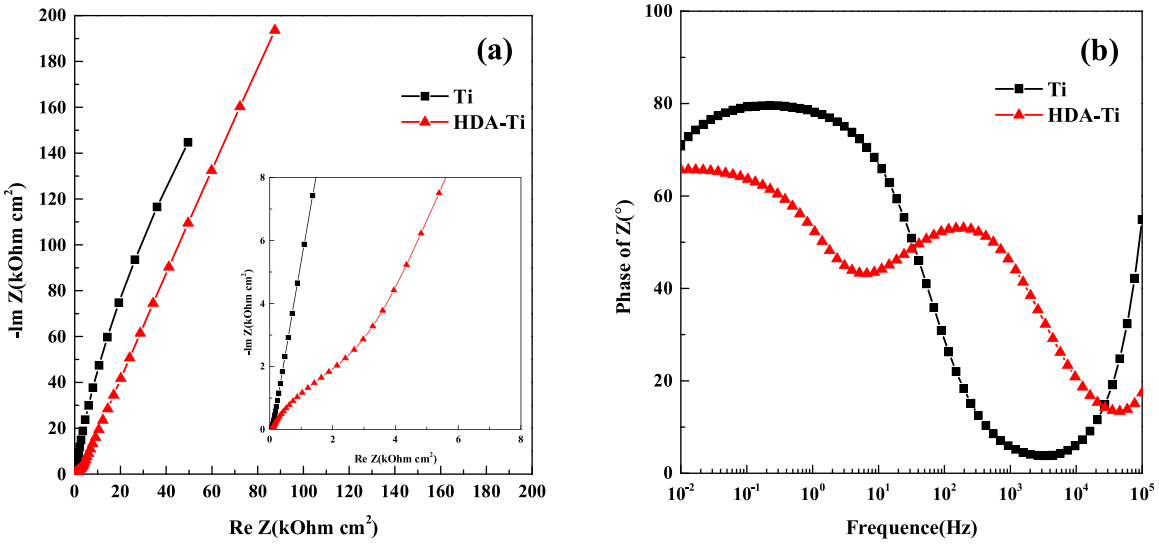

Fig. 9. Electrochemical impedance spectra of specimens in 0.9 wt% NaCl solution: (a) Nyquist plots and (b) Bode plots.

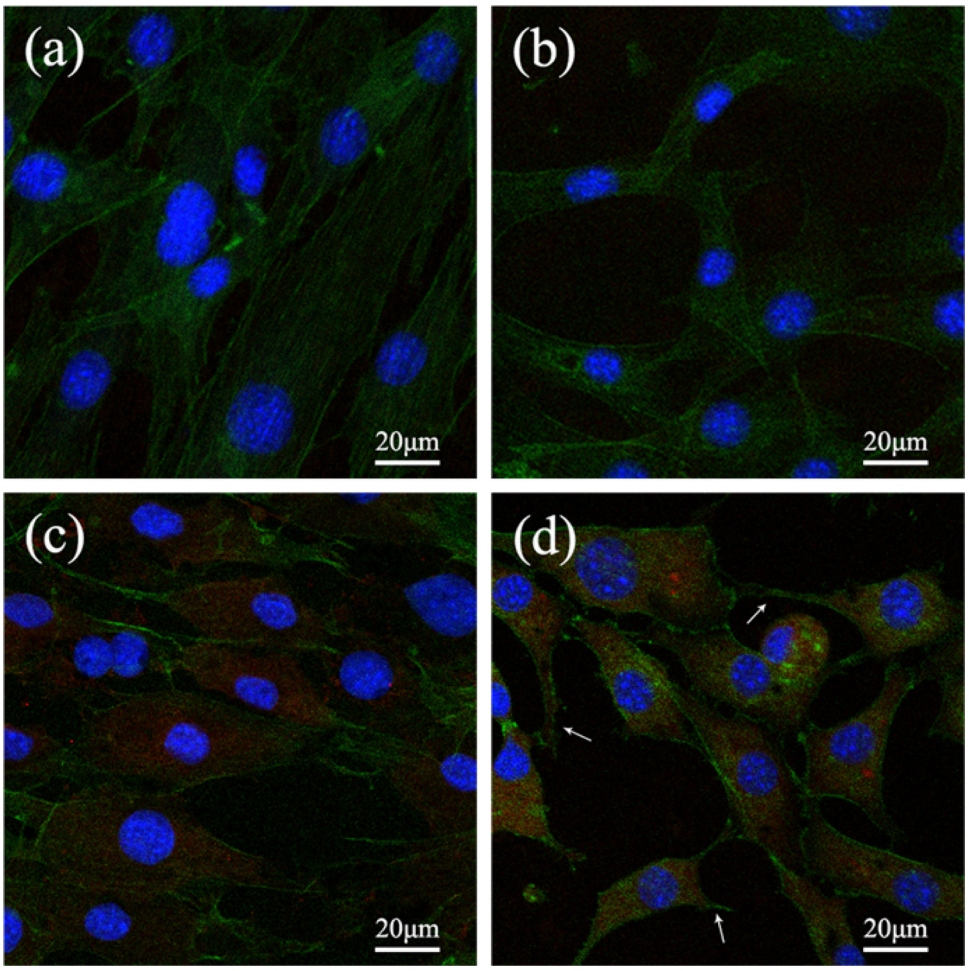

Fig. 11. Fluorescence images of MSCs adhered to (a) Ti, (b) H-Ti, (c) HD-Ti and (d) HDA-Ti. Cells were stained with cell nuclei (blue), actin filaments (green) and vinculin (red) in this study. (For interpretation of the references to color in this figure legend, the reader is referred to the web version of this article).

Table 1
Chemical composition of each samples measured by XPS.

Atomic%							
Specimen	Ti2p	O1s	C1s	N1s	Ca2p	P2p	N/C
Ti	4.93	10.90	71.23				
H	35.88	44.41	19.71				
HD	40.47	8.49	82.15	9.35			0.1138

tals. Therefore, both the electrostatic potential interaction and the specific structure of HD-Ti contribute to the formation of apatite.

To demonstrate the successful formation of each layer onto the Ti substrates, XPS was performed. Fig. 4 shows the XPS spectra for Ti, H-Ti, HD-Ti and HDA-Ti, the elemental compositions of each layer are listed in Table 1. The uncoated Ti consisted of three elements of Ti, C and O. The presence of carbon was due to environmental contamination. Ti was always polluted by hydrocarbon adsorption from the ambient, because of its reactivities, which has been observed in several reports [29]. After anodization, the intensities of Ti (2p, 3s, 3p) and O (1s) peaks were greatly increased, which indicated the formation of a TiO_2 layer on the Ti substrates [30]. For HD-Ti, the peaks for N (1s) and C (1s) were enhanced and yielded a nitrogen-carbon ratio (N/C) of 0.11, which is close to the theoretical ratio of PDA (0.125) [15]. This revealed that the polydopamine successfully coated on the substrates. The presence of Ca and P on HDA-Ti implied the formation of calcium-phosphate compound.

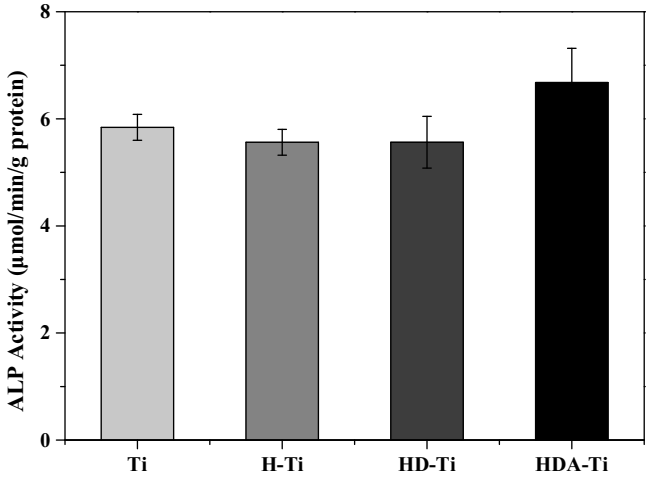

Fig. 12. ALP activity of MC3T3 cells after culturing for 2 days on the samples (Ti, H-Ti, HD-Ti and HDA-Ti).

The thin film XRD patterns for the four different types of coatings are shown in Fig. 5. Strong diffraction peaks associated with the anatase and rutile TiO_2 were detected after the anodization treatment. Compared to the rest groups, the peaks observed for HDA-Ti proved that the mineral depositing on the substrate was crystalline hydroxyapatite, which is consistent with the previous

Table 2
Electrochemical impedance parameters for Ti and HDA-Ti samples in 0.9 wt% NaCl.

Sample	R_s Ω cm^2	R_c Ω cm^2	Q_c F cm^{-2}	n_c	R_o Ω cm^2	Q_o F cm^{-2}	n_o
Ti	71.33	1.148×10^6	7.629×10^{-5}	0.8863	–	–	–
HDA-Ti	64.78	7.067×10^6	3.701×10^{-5}	0.7512	2592	1.726×10^{-5}	0.7028

studies [31,32]. The composition of the coating was further investigated by FTIR spectroscopy (Fig. 6). The peaks assigned to PO_4^{3-} at 1019 and 962 cm^{-1} are typical indications of hydroxyapatite. The broad band at 1103 and 1635 cm^{-1} are attributed to the different bonds of polydopamine. Additionally, weak peaks assigned to CO_3^{2-} were observed in the spectra because of its partial substitution of PO_4^{3-} during the apatite formation process.

When inside a human body, the implant firstly contacts with tissue fluid, thus, the surface hydrophilicity of biomaterials is an important factor influencing cell response. Here, the static water contact angle was tested to evaluate the hydrophilicity, and the water contact angle of each specimen is shown in Fig. 7. The anodization treatment had no significant influence on the surface hydrophilicity as compared with the Ti substrate. After coated with PDA layer, the HD-Ti was more hydrophilic than the H-Ti with the contact angle about 51°, which is consistent with theoretical value of pure PDA film [15]. However, with the formation of hydroxyapatite, the contact angle of HDA-Ti largely decreased and a better surface wettability was obtained, which may be beneficial for a more ideal biological response [33].

3.2. Corrosion resistance in a 0.9 wt% NaCl solution

Potentiodynamic polarization studies for uncoated and HDA modified surface were performed to assess the corrosion resistance in 0.9 wt% NaCl solution as is shown in Fig. 8. It was clear that the corrosion potential value corresponding to HDA-Ti was more ennobled than Ti substrate, which implied the improvement corrosion of HDA surface. Another fact to evaluate the anti-corrosion performance was the passive state, both of two surfaces had a broad passivity domain, however, the treated sample had the current densities in all passive domain lower than that of untreated Ti which revealed a better corrosion resistance. The result was superior to the research of Benea et al. [34] who obtained lower current densities only near body potential in passive range of the Ti–6Al–4V alloy by anodic oxidation and hydroxyapatite electrodeposition.

The EIS measurements were always investigated to account for the kinetics of corrosion process [35]. Fig. 9 shows the Nyquist and Bode plots of Ti and HDA-Ti samples in 0.9 wt% NaCl solution. The Nyquist plot of HDA-Ti represented two loops in Fig. 9a, which could be related to the formation of double layered oxide by anodization that are the inner dense and compact layer and the outer porous layer produced by a dielectric breakdown [36,37]. Based on the different physical structure of specimens and the phase shift plots, two time constants of HDA-Ti surface and single of Ti were used to fit the EIS spectra, and the suitable equivalent circuits for two surfaces are present in Fig. 10a and b, respectively. R_s was the resistance of electrolyte solution, R_c and Q_c were the resistance and the constant phase element of compact oxide layer, R_o and Q_o represented the resistance and the constant phase element of the outer layer, including porous TiO_2 layer and polydopamine layer, here, the hydroxyapatite layer was too loosened to be neglected. The fitting values were calculated and given in Table 2. It can be seen that the R_c corresponding to Ti is 1.148×10^6 Ω cm^2 while HDA-Ti is 7.067×10^6 Ω cm^2, the variation of R_c was attributed to that the inner dense layer by anodization of HDA-Ti had better corrosion resistance than the passive film of Ti that formed in the air spontaneously. R_o corresponding to the HDA-Ti was 2592 Ω cm^2, which represented the contribution of porous TiO_2 and polydopamine to the improvement of corrosion resistance.

3.3. Cell response

Fig. 11 shows the adhesion characteristics of MC3T3-E1 cells via immunofluorescence staining, MC3T3-E1 cells were stained with nuclei (blue), actin filaments (green) and vinculin (red) after two days of incubation. Compared with Ti and H-Ti, the MC3T3 cells response on HD-Ti and HDA-Ti exhibited greater cell spreading, and a clear filopodial extension morphology on HDA-Ti was observed, as is indicated by the arrows. Cell filopodia, the main structures in cell growth cones, contain bunches of actin filaments, which provide cytoskeleton support and link with the cell membrane. The receptors and molecules on cell membrane are crucial for cell growth and guidance [38]. Therefore, the results revealed that nano lath-like structure of hydroxyapatite on HDA-Ti stimulated faster cell spreading. Similarly, more vinculin in the cytoplasm of cells cultured on HD-Ti and HDA-Ti were observed compared with those on Ti and H-Ti. Vinculin, an intracellular protein responsible for the functional link of focal adhesions to the actin cytoskeleton, is widely used to evaluate cell adhesion and cytoskeletal development [39]. Greater expression of vinculin demonstrated that the surface of HD-Ti and HDA-Ti facilitated cell adhesion.

Fig. 12 shows the ALP activities of MC3T3 cells after culturing for 2 days on different substrates. Compared with uncoated Ti, H-Ti showed no improvement in ALP activity (a relatively small reduction in activity was observed), and the same trend was observed on HD-Ti. However, the ALP activity of HDA-Ti was significantly improved over that of the other three substrates. The ALP activity of cells is often monitored to evaluate the differentiation function of osteoblasts [40,41]. Therefore, the results demonstrated that the differentiation behavior of the cells was strongly affected by the type of coating treatment. In particular, when the sample was coated with HA, the differentiated function of MC3T3 cells was significantly improved. In combination with the results of cell adhesion, it was concluded that HDA-Ti with excellent cell adhesion and differentiated function showed good in vitro cytocompatibility.

A number of experiments have been investigated for the each layer in our study, including morphology, hydrophilicity, corrosion resistance and the biological effects, there are still some questions to be solved. For example, although some researchers have been proved that the hierarchical biocomposites through layer-by-layer assembly of PDA and HA on Ti have a good interfacial stability [18], the adhesion ability of HA layer on HD-Ti surface remains unknown, and whether the porous structure of anodized Ti made difference to the interfacial adhesion is also worth exploring. In addition, the HA layer produced by immersion is always loosened and irregular [17,18], the present study is no exception, thus a further research on how to deposit a relatively smooth HA layer in SBF solution still waits to be resolved.

4. Conclusions

In this study, we fabricated a simple and fast method to form hydroxyapatite on Ti by immersing PDA/anodized Ti into 1.5× SBF. The HD-Ti displayed the best growth of hydroxyapatite owing to the porous and hydroxyl-riched surface. After being coated with HA, the HDA-Ti surface exhibited excellent corrosion resistance and hydrophilicity. The results of in vitro tests suggested that the incor-

poration of HA on HD-Ti promoted the adhesion of MC3T3-E1 cells, as well as an increase in ALP activity.

Acknowledgements

This work is supported by the National Natural Science Foundation of China (Nos. 51222106 and 81371183), the Fundamental Research Funds for the Central Universities (No. 230201306500002) and National Basic Research Program of China (973 Program) (No. 2014CB643300).

References

[1] C.-S. Chen, Y.-L. Tsao, D.-J. Wang, S.-F. Ou, H.-Y. Cheng, Y.-C. Chiang, K.-L. Ou, Research on cell behavior related to anodized and hydrothermally treated titanium surface, Appl. Surf. Sci. 271 (2013) 1–6.
[2] L.T. Duarte, S.R. Biaggio, R.C. Rocha-Filho, N. Bocchi, Surface characterization of oxides grown on the Ti–13Nb–13Zr alloy and their corrosion protection, Corros. Sci. 72 (2013) 35–40.
[3] I.S. Park, T.G. Woo, W.Y. Jeon, H.H. Park, M.H. Lee, T.S. Bae, K.W. Seol, Surface characteristics of titanium anodized in the four different types of electrolyte, Electrochim. Acta 53 (2007) 863–870.
[4] C.Y. Chien, T.Y. Liu, W.H. Kuo, M.J. Wang, W.B. Tsai, Dopamine-assisted immobilization of hydroxyapatite nanoparticles and RGD peptides to improve the osteoconductivity of titanium, J. Biomed. Mater. Res. A 101 (2013) 740–747.
[5] J. Wu, Y.-q. Guo, G.-f. Yin, H.-q. Chen, Y. Kang, Induction of osteoconductivity by BMP-2 gene modification of mesenchymal stem cells combined with plasma-sprayed hydroxyapatite coating, Appl. Surf. Sci. 255 (2008) 336–339.
[6] C.-Y. Chien, W.-B. Tsai, Poly(dopamine)-assisted immobilization of Arg-Gly-Asp peptides, hydroxyapatite, and bone morphogenic protein-2 on titanium to improve the osteogenesis of bone marrow stem cells, ACS Appl. Mater. Interfaces 5 (2013) 6975–6983.
[7] H. Liu, P. Xi, G. Xie, Y. Shi, F. Hou, L. Huang, F. Chen, Z. Zeng, C. Shao, J. Wang, Simultaneous reduction and surface functionalization of graphene oxide for hydroxyapatite mineralization, J. Phys. Chem. C 116 (2012) 3334–3341.
[8] X. Nie, A. Leyland, A. Matthews, Deposition of layered bioceramic hydroxyapatite/TiO_2 coatings on titanium alloys using a hybrid technique of micro-arc oxidation and electrophoresis, Surf. Coat. Technol. 125 (2000) 407–414.
[9] S.W. Myung, Y.M. Ko, B.H. Kim, Effect of plasma surface functionalization on preosteoblast cells spreading and adhesion on a biomimetic hydroxyapatite layer formed on a titanium surface, Appl. Surf. Sci. 287 (2013) 62–68.
[10] K. De Groot, R. Geesink, C. Klein, P. Serekian, Plasma sprayed coatings of hydroxylapatite, J. Biomed. Mater. Res. 21 (1987) 1375–1381.
[11] H.-W. Kim, Y.-H. Koh, L.-H. Li, S. Lee, H.-E. Kim, Hydroxyapatite coating on titanium substrate with titania buffer layer processed by sol–gel method, Biomaterials 25 (2004) 2533–2538.
[12] K. Lee, H.-C. Choe, B.-H. Kim, Y.-M. Ko, The biocompatibility of HA thin films deposition on anodized titanium alloys, Surf. Coat. Technol. 205 (2010) S267–S270.
[13] D.-Y. Kim, M. Kim, H.-E. Kim, Y.-H. Koh, H.-W. Kim, J.-H. Jang, Formation of hydroxyapatite within porous TiO_2 layer by micro-arc oxidation coupled with electrophoretic deposition, Acta Biomater. 5 (2009) 2196–2205.
[14] C. Wu, P. Han, X. Liu, M. Xu, T. Tian, J. Chang, Y. Xiao, Mussel-inspired bioceramics with self-assembled Ca-P/polydopamine composite nanolayer: preparation, formation mechanism, improved cellular bioactivity and osteogenic differentiation of bone marrow stromal cells, Acta Biomater. 10 (2014) 428–438.
[15] H. Lee, S.M. Dellatore, W.M. Miller, P.B. Messersmith, Mussel-inspired surface chemistry for multifunctional coatings, Science 318 (2007) 426–430.
[16] F. Bernsmann, V. Ball, F. Addiego, A. Ponche, M. Michel, J.J.d.A. Gracio, V. Toniazzo, D. Ruch, Dopamine- melanin film deposition depends on the used oxidant and buffer solution, Langmuir 27 (2011) 2819–2825.
[17] J. Ryu, S.H. Ku, H. Lee, C.B. Park, Mussel-inspired polydopamine coating as a universal route to hydroxyapatite crystallization, Adv. Funct. Mater. 20 (2010) 2132–2139.
[18] Y. Wu, X. Liu, Y. Li, M. Wang, Surface-adhesive layer-by-layer assembled hydroxyapatite for bioinspired functionalization of titanium surfaces, RSC Adv. 4 (2014) 44427–44433.
[19] Y.-T. Liu, K.-C. Kung, C.-Y. Yang, T.-M. Lee, T.-S. Lui, Engineering three-dimensional structures using bio-inspired dopamine and strontium on titanium for biomedical application, J. Mater. Chem. B 2 (2014) 7927–7935.
[20] Y.-X. Liu, X.-J. Wang, J. Lu, C.-B. Ching, Influence of the roughness, topography, and physicochemical properties of chemically modified surfaces on the heterogeneous nucleation of protein crystals, J. Phys. Chem. B 111 (2007) 13971–13978.
[21] B. Yang, M. Uchida, H.-M. Kim, X. Zhang, T. Kokubo, Preparation of bioactive titanium metal via anodic oxidation treatment, Biomaterials 25 (2004) 1003–1010.
[22] T. Kokubo, H. Takadama, How useful is SBF in predicting in vivo bone bioactivity? Biomaterials 27 (2006) 2907–2915.
[23] W.-E. Yang, H.-H. Huang, Improving the biocompatibility of titanium surface through formation of a TiO_2 nano-mesh layer, Thin Solid Films 518 (2010) 7545–7550.
[24] Y. Bai, S. Li, F. Prima, Y. Hao, R. Yang, Electrochemical corrosion behavior of Ti–24Nb–4Zr–8Sn alloy in a simulated physiological environment, Appl. Surf. Sci. 258 (2012) 4035–4040.
[25] D. Upadhyay, M.A. Panchal, R. Dubey, V. Srivastava, Corrosion of alloys used in dentistry: a review, Mater. Sci. Eng. A 432 (2006) 1–11.
[26] D. Wei, Y. Zhou, D. Jia, Y. Wang, Characteristic and in vitro bioactivity of a microarc-oxidized TiO_2-based coating after chemical treatment, Acta Biomater. 3 (2007) 817–827.
[27] D. Wei, Y. Zhou, D. Jia, Y. Wang, Structure of calcium titanate/titania bioceramic composite coatings on titanium alloy and apatite deposition on their surfaces in a simulated body fluid, Surf. Coat. Technol. 201 (2007) 8715–8722.
[28] J. Jiang, L. Zhu, L. Zhu, B. Zhu, Y. Xu, Surface characteristics of a self-polymerized dopamine coating deposited on hydrophobic polymer films, Langmuir 27 (2011) 14180–14187.
[29] M. Lai, K. Cai, L. Zhao, X. Chen, Y. Hou, Z. Yang, Surface functionalization of TiO_2 nanotubes with bone morphogenetic protein 2 and its synergistic effect on the differentiation of mesenchymal stem cells, Biomacromolecules 12 (2011) 1097–1105.
[30] A.O.T. Patrocínio, E.B. Paniago, R.M. Paniago, N.Y.M. Iha, XPS characterization of sensitized n-TiO_2 thin films for dye-sensitized solar cell applications, Appl. Surf. Sci. 254 (2008) 1874–1879.
[31] H. Farnoush, A.A. Bastami, A. Sadeghi, J.A. Mohandesi, F. Moztarzadeh, Tribological and corrosion behavior of friction stir processed Ti-CaP nanocomposites in simulated body fluid solution, J. Mech. Behav. Biomed. Mater. 20 (2013) 90–97.
[32] A. Yanovska, A. Stanislavov, L. Sukhodub, V. Kuznetsov, V.Y. Illiashenko, S. Danilchenko, L. Sukhodub, Silver-doped hydroxyapatite coatings formed on Ti–6Al–4V substrates and their characterization, Mater. Sci. Eng. C 36 (2014) 215–220.
[33] P. Thevenot, W. Hu, L. Tang, Surface chemistry influence implant biocompatibility, Curr. Top. Med. Chem. 8 (2008) 270.
[34] L. Benea, E. Mardare-Danaila, M. Mardare, J.-P. Celis, Preparation of titanium oxide and hydroxyapatite on Ti–6Al–4V alloy surface and electrochemical behaviour in bio-simulated fluid solution, Corros. Sci. 80 (2014) 331–338.
[35] M. Babaei, C. Dehghanian, M. Vanaki, Effect of additive on electrochemical corrosion properties of plasma electrolytic oxidation coatings formed on CP Ti under different processing frequency, Appl. Surf. Sci. 357 (2015) 712–720.
[36] S.A. Fadl-Allah, R.M. El-Sherief, W.A. Badawy, Electrochemical formation and characterization of porous titania (TiO_2) films on Ti, J. Appl. Electrochem. 38 (2008) 1459–1466.
[37] M. Fazel, H. Salimijazi, M. Golozar, A comparison of corrosion, tribocorrosion and electrochemical impedance properties of pure Ti and Ti6Al4V alloy treated by micro-arc oxidation process, Appl. Surf. Sci. 324 (2015) 751–756.
[38] H.-H. Huang, C.-P. Wu, Y.-S. Sun, T.-H. Lee, Improvements in the corrosion resistance and biocompatibility of biomedical Ti–6Al–7Nb alloy using an electrochemical anodization treatment, Thin Solid Films 528 (2013) 157–162.
[39] J.D. Humphries, P. Wang, C. Streuli, B. Geiger, M.J. Humphries, C. Ballestrem, Vinculin controls focal adhesion formation by direct interactions with talin and actin, J. Cell Biol. 179 (2007) 1043–1057.
[40] F. Zhou, K. Qiu, H. Li, T. Huang, B. Wang, L. Li, Y. Zheng, Screening on binary Zr–1X (X = Ti, Nb, Mo, Cu, Au, Pd, Ag, Ru, Hf and Bi) alloys with good in vitro cytocompatibility and magnetic resonance imaging compatibility, Acta Biomater. 9 (2013) 9578–9587.
[41] K. Qiu, Y. Liu, F. Zhou, B. Wang, L. Li, Y. Zheng, Y. Liu, Microstructure, mechanical properties, castability and in vitro biocompatibility of Ti–Bi alloys developed for dental applications, Acta Biomater. 15 (2015) 254–265.